

Renormalization group fixed points, universal phase diagram, and $1/N$ expansion for quantum liquids with interactions near the unitarity limit

Predrag Nikolić and Subir Sachdev

Department of Physics, Harvard University, Cambridge MA 02138

(Dated: February 6, 2008)

It has long been known that particles with short-range *repulsive* interactions in spatial dimension $d = 1$ form universal quantum liquids in the low density limit: all properties can be related to those of the spinless free Fermi gas. Previous renormalization group (RG) analyses demonstrated that this universality is described by an RG fixed point, infrared stable for $d < 2$, of the zero density gas. We show that for $d > 2$ the *same* fixed point describes the universal properties of particles with short-range *attractive* interactions near a Feshbach resonance; the fixed point is now infrared unstable, and the relevant perturbation is the detuning of the resonance. Some exponents are determined exactly, and the same expansion in powers of $(d - 2)$ applies for scaling functions for $d < 2$ and $d > 2$. A separate exact RG analysis of a field theory of the particles coupled to ‘molecules’ finds an alternative description of the same fixed point, with identical exponents; this approach yields a $(4 - d)$ expansion which agrees with the recent results of Nishida and Son (Phys. Rev. Lett. **97**, 050403 (2006)). The existence of the RG fixed point implies a universal phase diagram as a function of density, temperature, population imbalance, and detuning; in particular, this applies to the BEC-BCS crossover of fermions with *s*-wave pairing. Our results open the way towards computation of these universal properties using the standard field-theoretic techniques of critical phenomena, along with a systematic analysis of corrections to universality. We also propose a $1/N$ expansion (based upon models with $\text{Sp}(2N)$ symmetry) of the fixed point and its vicinity, and use it to obtain results for the phase diagram.

I. INTRODUCTION

The study of ultracold atomic gases has drawn renewed attention to interacting quantum gases in regimes where their properties are independent of all microscopic details of the interaction between the atoms. This happens when the scattering cross-section between two atoms reaches its unitarity limit.

The simplest example of this phenomenon is the dilute Bose gas with short-range repulsive interactions in spatial dimension $d = 1$ where, in fact, the properties are generically universal. It is a well-known property of quantum-mechanical scattering in one dimension that for any generic short-range potential, the S matrix for two particle scattering reaches its unitarity limit value of -1 in the limit of zero momentum transfer. However, the strongly interacting Bose gas with $S = -1$ can be reinterpreted¹ as a *free* Fermi gas (the ‘Tonks’ gas), allowing easy computation of at least the thermodynamic properties. Correlation functions are much harder to compute, especially at finite temperature and unequal times, but much theoretical effort has been expended in this direction.^{2,3,4,5} Experimental studies of Tonks gas behavior have also appeared.⁶

No generic unitarity limit scattering is obtained in $d = 3$. In this case, we usually have the limit $S = 1$ for low momentum, implying that sufficiently slowly moving particles do not scatter. However, upon fine-tuning the strength of an attractive interaction, it is possible to obtain unitarity limit scattering across a Feshbach resonance.^{7,8,9} Near a Feshbach resonance, the *s*-wave

scattering amplitude, f_0 , takes the form¹⁰

$$f_0 = \frac{1}{\nu - ik} \quad (1)$$

where k is the momentum transfer, $S = 1 + 2ikf_0$, and ν is the ‘detuning’ across the resonance (it is related to the scattering length, a , by $\nu = -1/a$). The resonance occurs at $\nu = 0$, and notice then that $S = -1$, the unitarity limit. We will be interested here in *broad* Feshbach resonances, where Eq. (1) holds over all the momenta of interest in a quantum gas. For a gas with density n , a resonance is broad if the $\mathcal{O}(k^2)$ corrections to the denominator of Eq. (1) are negligible at the characteristic momentum $n^{1/3}$ (we use $\hbar = 1$ throughout). Notice then that the width condition on the Feshbach resonance, is actually a diluteness condition on the quantum gas, and any Feshbach resonance is ‘broad’ for a sufficiently dilute gas.

This paper demonstrates that a unified understanding of the distinct universal properties of the quantum gases in $d = 1$ and $d = 3$ can be obtained in a field-theoretic renormalization group (RG) analysis. The RG approach was used previously^{3,5,11,12} for the repulsive Bose gas in $d < 2$, and here we demonstrate that a direct generalization applies to a wide class of quantum liquids in general d . We will use the structure of an RG fixed point to argue that there is a *universal phase diagram* as a function of relevant perturbations away from the fixed point: these perturbations are the temperature, the detuning away from the Feshbach resonance, and the density imbalance for a two-component quantum gas. Our claims of universality are stronger than previous ones which applied only at the resonance.^{7,8,9} In particular, questions on the nature of the phases, including the existence of exotic

gapless superfluid states, have a unique and universal answer for a broad Feshbach resonance. We will also obtain explicit results for this phase diagram, and for associated universal scaling functions, for the two-component Fermi gas in $d = 3$ with s -wave pairing using a $1/N$ expansion of a model with $\text{Sp}(2N)$ symmetry. In particular, we obtain results on the equation of state for the normal state with unbalanced densities and two Fermi surfaces.

The form of our universal phase diagram has similarities to work by Sheehy and Radzihovsky^{13,14} (and related work by others¹⁵) where they departed from the narrow resonance limit in an expansion in the resonance width. We discover the same phases and transitions between them, except the possible non-uniform phases which are not a focus of this paper. The main advance in our work is a systematic treatment of the broad resonance limit, which is experimentally relevant, and in which universality applies. Universality has also been explored using a different RG analysis in Ref. 16: they do not give a “critical phenomena” interpretation of the results, which we claim below yield the most direct interpretation and computation tools for identifying universal behavior.

The previous study^{3,5,11,12} of the dilute Bose gas began with an RG analysis of the field theory of the zero density gas¹⁷ at chemical potential $\mu = 0$, considered as a quantum critical point between the vacuum state for $\mu < 0$, and the finite density ground state for $\mu > 0$. Interactions between a pair of particles created out of the vacuum are characterized by a coupling u (defined more precisely in the body of the paper), and this coupling was shown to obey the *exact* field-theoretic RG equation

$$\frac{du}{d\ell} = (2 - d)u - \frac{u^2}{2} \quad (2)$$

under a rescaling of length scales by a factor of e^ℓ , and a dynamic exponent $z = 2$. As we will review later, this RG equation applies equally to two-body interactions between particles with arbitrary statistics and masses. As shown in Fig. 1, for $d < 2$, this RG equation has an infrared stable fixed point at $u^* > 0$. It was argued^{5,11,12} that this fixed point interaction which describes unitarity scattering. The chemical potential, μ , is a relevant perturbation at this fixed point, and its scaling dimension, and RG flow can also be determined exactly. A standard¹⁸ field-theoretic analysis then allowed computation⁵ of all universal properties of the $\mu \neq 0$ Bose gas in $d < 2$, in an expansion which can be carried out to all orders in $u^* = 2(2 - d)$. The degree of difficulty of this computation is the same for thermodynamic and dynamic correlations. Practically speaking, this expansion is then useful for those physical properties which are difficult to access by the fermionization method in $d = 1$. In some cases, an exact computation is possible both in the fermionization approach, and also by resumming all orders in the $(2 - d)$ expansion, and exact agreement was obtained.³ A review of this approach to Bose and Fermi quantum liquids in $d < 2$ appears in Section II.

Let us now examine the RG equation (2) for $d > 2$.

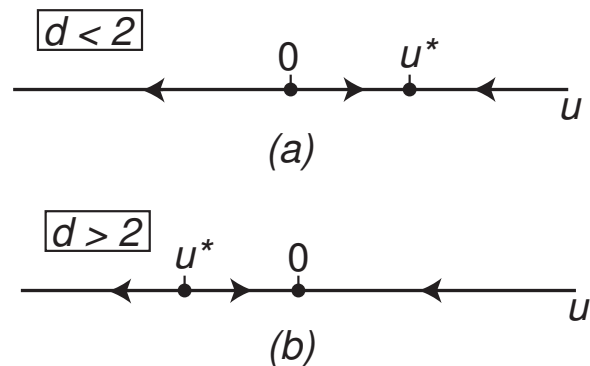


FIG. 1: The exact RG flow of Eq. (2), as discussed in Ref. 5. Here u is a measure of the short-range two-body interaction between the particles, and the RG applies in the limit of low density of either Bose, Fermi, or Bose-Fermi quantum liquids. (a) For $d < 2$, the infrared stable fixed point at $u = u^* > 0$ describes quantum liquids of either bosons or fermions with repulsive interactions which are generically universal in the low density limit. In $d = 1$ this fixed point is described by the spinless free Fermi gas (‘Tonks’ gas), for all statistics and spin of the constituent particles. (b) For $d > 2$, the infrared unstable fixed point at $u = u^* < 0$ describes the Feshbach resonance which obtains for the case of attractive interactions. The relevant perturbation $(u - u^*)$ corresponds to the detuning from the resonant interaction.

The flows are shown in Fig 1. Now there is an infrared *unstable* fixed point at a $u^* < 0$. We show here that this fixed point describes the Feshbach resonance of particles with attractive interactions. The unitarity of the scattering at this fixed point has also been pointed out independently in Ref. 19. The relevant perturbation $(u - u^*)$ is proportional to the detuning, ν , of the resonance. By an elementary computation of the eigenvalue of linear perturbations from the $u = u^*$ fixed point of Eq. (2) we therefore determine the exact scaling dimension

$$\dim[\nu] = d - 2 \quad (3)$$

The universal properties of the quantum liquid with $\nu \neq 0$ and $\mu \neq 0$ can now be determined by essentially the same renormalized theory earlier used for $d < 2$, and now becomes an expansion in $(d - 2)$. Indeed, as we will see in Section II, the earlier⁵ $(2 - d)$ expansions for scaling functions for $d < 2$, apply *unchanged* at resonance for $d > 2$. A shortcoming of this $(d - 2)$ expansion for the attractive Fermi gas is that the pairing amplitude is of order $\exp(1/u^*) \sim \exp(-1/(d - 2))$, and so all effects associated with superconductivity are non-perturbative.

Regardless of the ability to determine scaling functions in the $(d - 2)$ expansion, the flow equation (2), and its associated exponents are exact, and allow us to deduce some exact scaling forms associated with the RG fixed point in $d > 2$. For the two-component Fermi gas, we have already noted two relevant perturbations at the fixed point, the detuning ν and the chemical potential μ . For general d , we define the overall scale of ν by the

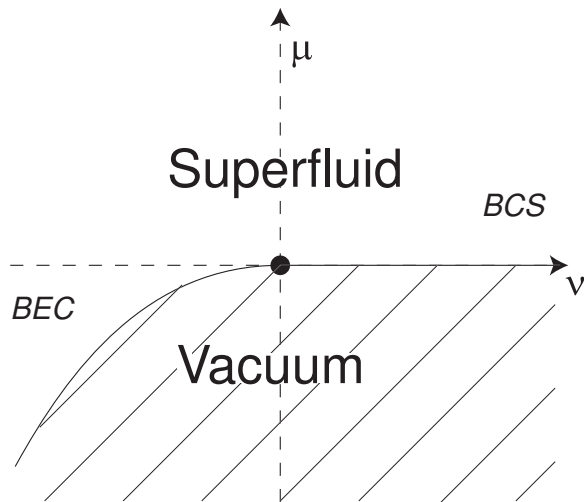


FIG. 2: Universal phase diagram at zero temperature ($T = 0$) and balanced densities ($h = 0$) for the two-component Fermi gas in $d = 3$. The vacuum state (shown hatched) has no particles, and is present for $\mu < 0$ and $\nu > 0$, or for $\nu < 0$ and $\mu < -\nu^2/(2m)$, where m is the mass of a fermion. The position of the $\nu < 0$ phase boundary is determined by the energy of the two-fermion bound state. The density of particles vanishes continuously at the second order quantum phase transition boundary of the superfluid phase, which is indicated by the thin continuous line. The quantum multicritical point at $\mu = \nu = h = T = 0$ (denoted by the filled circle) is the RG fixed point which is the basis for the analysis in this paper.

requirement that the s -wave scattering amplitude is proportional to $1/(\nu - (-k^2)^{(d-2)/2})$. The scaling dimension of μ is exactly 2. There is also a third relevant perturbation at the fixed point: a ‘field’ h conjugate to the density difference of the two species of fermions, which also has scaling dimension 2. From all this information, and the dynamic exponent $z = 2$, we can deduce one of our central results, a scaling form for the grand canonical free energy density \mathcal{F} (from the usual thermodynamic identity, $\mathcal{F} = -P$, the pressure) at a temperature T :

$$\mathcal{F} = (2m)^{d/2} T^{1+d/2} F_{\mathcal{F}} \left(\frac{\mu}{T}, \frac{h}{T}, \frac{\nu}{(2mT)^{(d-2)/2}} \right), \quad (4)$$

where m is the mass of one of the particles, and $F_{\mathcal{F}}$ is a universal scaling function whose three arguments extend over all real values (if the mass of the particles are distinct, the scaling function will also depend upon the ratio of the masses). For the two-component Fermi gas this universal scaling function contains all the information on the BEC-BCS crossover.^{20,21,22,23} The existence of this scaling form also implies that there is a universal phase diagram as a function of μ , ν , h , and T in the low density limit (or equivalently, for a broad resonance). Information on all the phases and phase transitions in this phase diagram is also contained in Eq. (4). At $h = 0$ and $T = 0$, the form of this universal phase diagram can be deduced exactly, and is shown in Fig. 2 for $d = 3$. There is a second-order quantum phase transition line separating

the zero density vacuum from the low density superfluid. The RG fixed point is a multicritical point on this line, and the whole phase diagram is constructed as a theory of relevant perturbations from this point. Note that there is no phase transition at finite density within the superfluid, only a smooth crossover between the BCS and BEC limits. However, there is a quantum critical point at zero detuning (at ‘resonance’) on the phase boundary, and we use this critical point as a point of departure to describe the entire phase diagram. We will present further results on this phase diagram in the body of the paper.

Given the limitations of the $(d - 2)$ expansion for obtaining useful approximations for the scaling function, the remainder of the paper presents alternative approaches to analyzing the fixed point described above. In Section III, we examine another field theory commonly used to describe a Feshbach resonance: a theory of mixed ‘atoms’ and ‘molecules’, with the ‘molecule’ corresponding to the bound state in the vicinity of the Feshbach resonance (the so-called ‘two-channel’ approach^{14,24}). As argued above, it is useful to perform an RG analysis in the limit of zero density, when the physics reduces to the quantum mechanics of few-particle scattering. The RG flow equations can now also be determined exactly, and are presented in Section III. They contain a fixed point, which, at first glance, appears distinct from that of Eq. (2). However, a careful analysis of its universal properties, such as scaling dimensions of operators, shows that they are identical to the results quoted above. The finite density field theory associated with this fixed point becomes weakly coupled when $(4 - d)$ is small. Consequently, a standard renormalized perturbative expansion now allows us to obtain universal properties in powers of $(4 - d)$. The universal results of the $(4 - d)$ expansion are equal to those obtained recently in the important work of Nishida and Son²⁵, who motivated the expansion from different considerations and use a different computational scheme. The special role of $d = 2$ and $d = 4$ was also discussed by Nussinov and Nussinov.²⁶ Our method streamlines the expansion $(4 - d)$ onto the standard approach used extensively for critical phenomena, and also opens the way to a systematic analysis of corrections to scaling by a consideration of irrelevant perturbations.

Further considerations on the structure of the $(4 - d)$ expansion shows that it also has some limitations in its range of validity. For the two component Fermi gas, the naive $(4 - d)$ expansion is restricted to being well within the superfluid state, or well within the normal state with one Fermi surface. A subtle redefinition of parameter scales^{25,27} is required to obtain an expansion for the 2 Fermi surface normal state. The latter is one of the most interesting new regimes discovered in recent experiments^{28,29}, and so an unrestricted analysis here would be useful.

With this motivation, in Section IV we introduce a *third* approach towards analyzing the finite density field theory at the RG fixed point of Eq. 2. This is based upon the $1/N$ expansion, where N is the number of particle

species. This expansion holds uniformly for general μ , ν , h , and T . For the two-component Fermi gas, the critical fixed point has $\text{Sp}(2N)$ symmetry, and the expansion is based upon that considered earlier in Ref. 30 well away from the Feshbach resonance.

We conclude this introduction by briefly discussing quantum liquids with attractive interactions in $d < 2$; these are not directly described by the fixed points discussed so far. In such systems, the ‘atomic’ constituents will bind to form ‘molecules’ and the resulting molecules could have repulsive interactions, leading eventually to the quantum liquid of the type discussed above for $d < 2$. The crossovers associated with this behavior will be described by an RG analysis which is a combination of that presented in Sections II and III—we need to explicitly include the interactions between the atoms and the molecules (relevant for $d < 2$), along with 3-point term allowing for a molecule to decay into two atoms (relevant for $d < 4$). We will not present the details of such an RG analysis here, but note that these considerations are entirely consistent with a recent analysis by Gurarie³¹ in $d = 1$ using Bethe ansatz methods.

II. RG FOR A FIELD THEORY OF ATOMS

We begin by considering the theory of the dilute Bose gas, from the perspective of a zero density quantum critical point, as discussed in Ref. 5. We consider a zero density theory at the chemical potential $\mu = 0$. This can be viewed as a quantum critical point between the finite density phase with $\mu > 0$, and the empty vacuum ground state for $\mu < 0$. The critical theory of this quantum critical point of a boson, ψ , is

$$\mathcal{S}_c^b = \int d\tau d^d x \left\{ \psi^\dagger \left(\frac{\partial}{\partial \tau} - \frac{\nabla^2}{2m} \right) \psi + \frac{u_0}{2} \psi^\dagger \psi^\dagger \psi \psi \right\}. \quad (5)$$

The RG analysis of the zero density theory does not depend upon the statistics of the particles, so we also consider in parallel a theory of two-component fermions, ψ_σ , $\sigma = 1, 2$. The critical theory is

$$\mathcal{S}_c^f = \int d\tau d^d x \left\{ \psi_\sigma^\dagger \left(\frac{\partial}{\partial \tau} - \frac{\nabla^2}{2m} \right) \psi_\sigma + u_0 \psi_1^\dagger \psi_2^\dagger \psi_2 \psi_1 \right\}. \quad (6)$$

The single particle self-energy is identically zero at $T = 0$ because the vacuum state contains no particles. Consequently, we can perform an RG transformation with the exact dynamic critical exponent $z = 2$, and obtain the exact scaling dimension

$$\dim[\psi] = \dim[\psi_\sigma] = d/2. \quad (7)$$

Despite the trivial nature of the vacuum at $T = 0$, there is a non-trivial RG transformation of the two body interaction u_0 . This comes entirely from the ladder diagram of repeated two-particle scattering. Defining a

renormalized dimensionless coupling u by

$$u_0 = \frac{\kappa^{2-d} Z_4}{2m S_d} u, \quad (8)$$

where κ is a renormalization momentum scale, $S_d = 2/(\Gamma(d/2)(4\pi)^{d/2})$ is the standard phase space factor, and Z_4 is the renormalization constant. The ladder diagrams lead to the exact result

$$Z_4^{-1} = 1 - \frac{u}{2-d} \quad (9)$$

in the minimal subtraction scheme. From this, we obtain the exact RG β function for u presented earlier in Eq. (2), upon rescaling κ by a factor of e^ℓ .

Now we include relevant operators away from this fixed point (apart from $(u - u^*)$ for $d > 2$). For the single-component Bose gas, there is only one such term, the chemical potential

$$\mathcal{S}_{bp} = \int d\tau d^d x \left\{ -\mu \psi^\dagger \psi \right\}. \quad (10)$$

It is easy to see that an insertion of \mathcal{S}_p acquires no operator renormalization at the zero density critical point, and so from Eq. (7) we conclude that

$$\dim[\mu] = 2. \quad (11)$$

For the two-component Fermi gas, we have an additional relevant perturbation corresponding to the difference in chemical potential of the two species:

$$\mathcal{S}_{fp} = \int d\tau d^d x \left\{ \begin{array}{l} -\mu(\psi_1^\dagger \psi_1 + \psi_2^\dagger \psi_2) \\ -h(\psi_1^\dagger \psi_1 - \psi_2^\dagger \psi_2) \end{array} \right\}, \quad (12)$$

and again we have

$$\dim[h] = 2 \quad (13)$$

Now let us examine the universal properties of the finite density $\mu \neq 0$ theory in the vicinity of the fixed point of Eq. (2). We will consider the cases $d < 2$ and $d > 2$ separately in the following subsections.

A. $d < 2$

The fixed point of Eq. (2) has repulsive interactions with $u^* = 0$.

The properties of the Bose gas at this fixed point were already considered in Refs. 5,11. As an example, we note the grand canonical free energy density at $T = 0$, *i.e.* the pressure P . From Eq. (4), we deduce that this obeys

$$P = C_d^b \mu (2m\mu)^{d/2} \quad (14)$$

where C_d^b is a universal number. A $(2-d)$ expansion for C_d^b was presented in Ref. 5, and the leading result is⁵

$$C_d^b = S_d \left(\frac{1}{4(2-d)} + \frac{2 \ln 2 - 1}{16} + \mathcal{O}(2-d) \right). \quad (15)$$

The corresponding universal properties of the two-component Fermi gas at the repulsive $u = u^*$ are also easy to work out. For simplicity, we present results only at $T = 0$ and $h = 0$. Then, the result (14) still applies, but with a different universal constant C_d^f . This is easily computed from the perturbation theory for the pressure of the two-component Fermi gas to the first order in u_0 :

$$P = 2 \int_0^{\sqrt{2m\mu}} \frac{d^d k}{(2\pi)^d} \left(\frac{k^2}{2m} - \mu \right) + u_0 \left[\int_0^{\sqrt{2m\mu}} \frac{d^d k}{(2\pi)^d} \right]^2 + \mathcal{O}(u_0^2) \quad (16)$$

The universal result is obtained by evaluating (16) at $u = u^*$ consistently to order $(2-d)$.

$$C_d^f = S_d \left(\frac{1}{2} - \frac{(2-d)}{8} + \mathcal{O}(2-d)^2 \right). \quad (17)$$

Of course, in both the Bose and Fermi cases considered in this subsection, we can obtain exact results in $d = 1$. The thermodynamics of both models are equivalent to the free, spinless, Fermi gas. Note that even the thermodynamics of the dilute two-component Fermi gas is given by the spinless Fermi gas. From this, we easily obtain

$$C_1^b = C_1^f = \frac{2}{3\pi} \quad (18)$$

B. $d > 2$

The fixed point of Eq. (2) is now at $u^* = -2(d-2) < 0$.

The Bose gas with such attractive interactions is unstable, and further interactions are needed to stabilize the theory: we will therefore not consider it further here.

The Fermi gas is stable and has universal properties that can be computed for small $(d-2)$. Indeed, the expansion described in Section II A applies *unchanged* also for $d > 2$. In particular, the pressure is still given by Eq. (17), and this agrees with a recent result²⁷ obtained while this paper was in preparation. Of course, as noted in Section I, this expansion knows nothing about pairing between the fermions, as such effects are²⁷ exponentially small in $1/(2-d)$.

III. RG FOR A FIELD THEORY OF ATOMS AND MOLECULES

This section will use the popular “two-channel” formulation of the Feshbach resonance^{14,24} to obtain an alternative field theoretic description of universal fixed point

of Eq. (2). In addition to the ‘elementary’ particles, $\psi_{1,2}$, we will also allow for a ‘composite’ molecule, Φ . For generality, we will now allow the masses of the ψ_σ particles to be possibly distinct, m_1 and m_2 . By Galilean invariance, the mass of the ‘composite’ particle is $m_1 + m_2$. The statistics of the two ψ_σ can be arbitrary—they can be Fermi-Fermi, Bose-Fermi³², or Bose-Bose³³. The ‘composite’ particle Φ is then, naturally, a boson, fermion, or a boson respectively.

Our analysis will find a ‘critical’ fixed point describing the unitarity limit theory. All exponents and scaling dimensions associated with the fixed point will turn out to be identical to those obtained for a seemingly distinct fixed point in Section II, suggesting that the two theories are in fact identical.

As in Section II, it is useful to begin with an RG analysis of the zero density ‘critical’ theory, which is presented in Section III A. The perturbations away from the critical point are considered in Section III B.

A. Zero density critical theory

The action of the critical theory is now

$$\begin{aligned} \mathcal{S}_c = \int d\tau d^d x \left\{ \psi_\sigma^\dagger \left(\frac{\partial}{\partial \tau} - \frac{\nabla^2}{2m_\sigma} \right) \psi_\sigma \right. \\ \left. + \Phi^\dagger \left(\frac{\partial}{\partial \tau} - \frac{\nabla^2}{2(m_1 + m_2)} + r_{0c} \right) \Phi \right. \\ \left. - g_0 \left(\Phi^\dagger \psi_1 \psi_2 + \psi_2^\dagger \psi_1^\dagger \Phi \right) + \dots \right\} \quad (19) \end{aligned}$$

Here r_{0c} is a cutoff-dependent bare “mass” term which has to be tuned to place the theory at its critical point *i.e.* describe the unitarity limit scattering. In dimensional regularization, $r_{0c} = 0$. A tree-level scaling analysis with $z = 2$ shows that

$$\dim[\psi_\sigma] = d/2 \quad ; \quad \dim[\Phi] = d/2 \quad ; \quad \dim[g_0] = (4-d)/2 \quad (20)$$

All other interactions are irrelevant for $d > 2$. The scaling dimension of g_0 naturally suggests that we perform a renormalization group analysis as an expansion in $(4-d)$.

It turns out that it is possible to perform an RG analysis *exactly*, to all orders in $(4-d)$. Most of the Feynman diagrams vanish because of the zero density of the particles. The only non-zero renormalization is a wavefunction renormalization of the composite particle Φ . The wavefunction renormalization is computed from the Φ Green’s function

$$G_\Phi(k, \omega) = \frac{1}{-i\omega + k^2/(2(m_1 + m_2)) + r_{0c} - \Sigma_\Phi(k, \omega)} \quad (21)$$

For the above theory, at $T = 0$, the exact expression for

the self energy is

$$\begin{aligned}\Sigma_{\Phi}(k, \omega) &= g_0^2 \int \frac{d\Omega}{2\pi} \int \frac{d^d p}{(2\pi)^d} \frac{1}{(-i\Omega + p^2/(2m_2))} \\ &\quad \times \frac{1}{(-i(\omega - \Omega) + (k - p)^2/(2m_1))} \\ &= g_0^2 \frac{\Gamma(1 - d/2)}{(4\pi)^{d/2}} \left[\frac{2m_1 m_2}{(m_1 + m_2)} \right]^{d/2} \\ &\quad \times \left[-i\omega + \frac{k^2}{2(m_1 + m_2)} \right]^{d/2 - 1}. \quad (22)\end{aligned}$$

In the last equation, we have dropped a constant cut-off dependent term which cancels against r_{0c} (additional subtractions are necessary for $d > 4$). We now define a renormalized coupling g by

$$g_0 = \kappa^{(4-d)/2} \left[\frac{2m_1 m_2}{(m_1 + m_2)} \right]^{-d/4} \frac{1}{\sqrt{Z_{\Phi} S_d}} g. \quad (23)$$

where Z_{Φ} allows for a non-trivial wavefunction renormalization of the Φ field. It is easy to check that additional self-energy and vertex corrections vanish in the zero density theory at $T = 0$, and so there is no wavefunction renormalization for the ψ_{σ} , nor an independent coupling constant renormalization of g_0 . In terms of g , we can expand the self energy to leading order in $(4 - d)$, and obtain

$$\Sigma_{\Phi}(k, \omega) = -\frac{g^2}{Z_{\Phi}(4-d)} \left[-i\omega + \frac{k^2}{2(m_1 + m_2)} \right] \quad (24)$$

Cancelling poles in the minimal subtraction scheme³⁴, we obtain the exact value of Z_{Φ} :

$$Z_{\Phi} = 1 - \frac{g^2}{(4-d)} \quad (25)$$

Using Eq. (23), we can compute the exact β function for g :

$$\frac{dg}{d\ell} = \frac{(4-d)}{2} g - \frac{g^3}{2}. \quad (26)$$

Also, from Eq. (25), we obtain for the anomalous dimension of the composite field Φ :

$$\eta(g) = g^2. \quad (27)$$

For $d < 4$, the RG flow equation Eq. (26) has an infrared *stable* fixed point at $g^* = \sqrt{4-d}$. At first sight, this may seem puzzling because in Section II we described the Feshbach resonance by an infrared *unstable* fixed point. However, this is just a matter of our restriction here to a particular critical manifold. We will see in Section III B, where we consider the full parameter space of the theory, that there is indeed an additional relevant operator here which corresponds to the relevant perturbation of Section II, and this is the detuning away from

the Feshbach resonance. The attractive flow towards the $g = g^*$ fixed point above corresponds to the $\mathcal{O}(k^2)$ corrections to the scattering amplitude we discussed below Eq. (1): the system can be assumed to be exactly at $g = g^*$ for a broad Feshbach resonance, while the irrelevant flows towards $g = g^*$ have to be included for a narrow resonance. As stated earlier, we restrict our computations here to the broad resonance.

The critical exponents are to be evaluated at the fixed point of Eq. (26). From this, we obtain the exact results

$$\eta = \eta(g^*) = (4-d) \ ; \ \dim[\Phi] = (d + \eta)/2 = 2. \quad (28)$$

This (along with Galilean invariance) implies that the Φ Green's function behaves like $G_{\Phi}^{-1} \sim [-i\omega + k^2/(2(m_1 + m_2))]^{1-\eta/2}$, which is, of course, the result already obtained in Eq. (22).

At this point, the above RG fixed point appears to bear little direct relation to the fixed point discussed in Section II. In the following subsection we show that the spectrum of eigenoperators of the two fixed points are identical, indicating that they describe the same universal physics.

B. Perturbations to finite density

Having obtained the critical theory \mathcal{S}_c , we can now look at all possible perturbations, and classify them according to their renormalization group eigenvalues. It turns out that there are 3 relevant perturbations, and all other perturbations are irrelevant. Anticipating the RG computation, we can arrange these perturbations into eigenoperators of the RG transformation as

$$\begin{aligned}\mathcal{S}_p = \int d\tau d^d x \left\{ -\mu(\psi_1^{\dagger}\psi_1 + \psi_2^{\dagger}\psi_2 + 2\Phi^{\dagger}\Phi) \right. \\ \left. + \delta\Phi^{\dagger}\Phi - h(\psi_1^{\dagger}\psi_1 - \psi_2^{\dagger}\psi_2) \right\} \quad (29)\end{aligned}$$

We can interpret the three relevant perturbations as the chemical potential, μ , a measure of the detuning away from unitary scattering, δ , and the ‘magnetic’ field, h , which breaks the symmetry between ψ_1 and ψ_2 . It is a simple matter to relate δ to the detuning ν in Eq. (1). The T matrix for scattering between ψ_1 and ψ_2 is equal to $g_0^2 G_{\Phi}$. We have to evaluate this on-shell, for incoming particles with momenta k_1 and k_2 , which then requires $G_{\Phi}(k = k_1 + k_2, \omega = -i(k_1^2/(2m_1) + k_2^2/(2m_2)))$ in the presence of a non-zero δ . Using Eq. (22) in $d = 3$, and comparing the result with Eq. (1), we conclude

$$\nu = \frac{2\pi(m_1 + m_2)}{m_1 m_2} \frac{\delta}{g_0^2} \quad (30)$$

The RG flow equations for the μ, ν, h perturbations are computed using the standard operator insertion methods.

restrict our attention here to a constant Φ , in which case

$$\begin{aligned} \frac{\mathcal{F}^{(0)}}{N} &= \frac{m\nu}{4\pi} |\Phi|^2 - \int \frac{d^3 p}{(2\pi)^3} \left[\right. \\ &T \ln \left(1 + e^{-\sqrt{(p^2/(2m)-\mu)^2+|\Phi|^2-h}/T} \right) \\ &+ T \ln \left(1 + e^{-\sqrt{(p^2/(2m)-\mu)^2+|\Phi|^2+h}/T} \right) \\ &\left. + \sqrt{\left(\frac{p^2}{2m} - \mu\right)^2 + |\Phi|^2} - \left(\frac{p^2}{2m} - \mu\right) \right]. \end{aligned} \quad (36)$$

The superscript on \mathcal{F} denotes that expression above is divergent in the ultraviolet. As discussed above, the momentum integral has to be evaluated in dimensional regularization, by a process of analytic continuation from a convergent result for $d < 2$ to $d > 2$. We do this by adding and subtracting $m|\Phi|^2/(p^2 + \Lambda^2)$ from the integrand, where Λ is an arbitrary momentum scale. Then, the subtracting integrand is explicitly convergent for $d = 3$, while the compensating term can be evaluated analytically by dimensional regularization. This yields

$$\begin{aligned} \frac{\mathcal{F}}{N} &= \left(\frac{m\nu}{4\pi} - \frac{m\Lambda\Gamma(1-d/2)}{(4\pi)^{d/2}} \right) |\Phi|^2 - \int \frac{d^3 p}{(2\pi)^3} \left[\right. \\ &T \ln \left(1 + e^{-\sqrt{(p^2/(2m)-\mu)^2+|\Phi|^2-h}/T} \right) \\ &+ T \ln \left(1 + e^{-\sqrt{(p^2/(2m)-\mu)^2+|\Phi|^2+h}/T} \right) \\ &\left. + \sqrt{\left(\frac{p^2}{2m} - \mu\right)^2 + |\Phi|^2} - \left(\frac{p^2}{2m} - \mu\right) - \frac{m|\Phi|^2}{p^2 + \Lambda^2} \right]. \end{aligned} \quad (37)$$

where the dimensionally regularized term can be evaluated directly in $d = 3$. It can now be checked that the above expression is independent of Λ , and is most easily evaluated at $\Lambda = 0$. The procedure above also shows that the subtraction is only needed for the $|\Phi|^2$ term, but not for any of the higher powers in Φ .

The phase diagram is determined by minimizing Eq. (37) with respect to Φ . The resulting free energy obeys Eq. (4), and so yields a universal phase diagram as a function of μ , h , ν and T . We will present results for aspects of this phase diagram, along with $1/N$ corrections, in the subsections below.

A. Superconductor to normal transition with increasing T

At sufficiently high T , it is always the case that $\langle \Phi \rangle = 0$. In this case, we can expand \mathcal{S}_Φ about $\Phi = 0$ for an arbitrary spatial and temporal dependence of Φ . To first order in $1/N$, we need to expand the action for Φ to fourth order:

$$\begin{aligned} \frac{\mathcal{S}_\Phi}{N} &= T \sum_{\omega_n} \int \frac{d^d k}{(2\pi)^d} K_2(k, \omega_n) \Phi^\dagger(k, \omega_n) \Phi(k, \omega_n) \\ &+ \frac{1}{2} \prod_{i=1}^3 \left(T \sum_{\omega_{in}} \int \frac{d^d k_i}{(2\pi)^d} \right) \tilde{K}_4(k_i, \omega_{in}) \Phi^\dagger(k_1, \omega_{1n}) \Phi^\dagger(k_2, \omega_{2n}) \Phi(k_3, \omega_{3n}) \\ &\quad \times \Phi(k_1 + k_2 - k_3, \omega_{1n} + \omega_{2n} - \omega_{3n}) \end{aligned} \quad (38)$$

Here

$$K_2(k, \omega_n) = \frac{m\nu}{4\pi} - \int \frac{d^d p}{(2\pi)^d} \left(\frac{1 - f[(p+k)^2/(2m) - \mu - h] - f[p^2/(2m) - \mu + h]}{-i\omega_n + p^2/(2m) + (p+k)^2/(2m) - 2\mu} - \frac{m}{p^2} \right) \quad (39)$$

where $f(\epsilon) = 1/(e^{\epsilon/T} + 1)$ is the Fermi function, and we have performed the dimensional regularization with the subtraction of the m/p^2 term. Also, we will only need \tilde{K}_4 when two of its arguments have zero momenta and frequency, in which case it equals $K_4(k, \omega_n)$, given by

$$\begin{aligned} K_4(k, \omega_n) &= \frac{1}{2} \int \frac{d^d p}{(2\pi)^d} \left[I \left((k-p)^2/(2m) - \mu - h, p^2/(2m) - \mu + h, \omega_n \right) \right. \\ &\quad \left. + I \left((k-p)^2/(2m) - \mu + h, p^2/(2m) - \mu - h, \omega_n \right) \right] \end{aligned} \quad (40)$$

where

$$\begin{aligned}
I(\epsilon_1, \epsilon_2, \omega_n) &= \frac{\tanh(\epsilon_1/(2T)) + \tanh(\epsilon_2/(2T))}{4\epsilon_2(\epsilon_1 + \epsilon_2 - i\omega_n)^2} \\
&+ \frac{\tanh(\epsilon_1/(2T)) + \tanh(\epsilon_2/(2T)) - (\epsilon_2/T)\operatorname{sech}^2(\epsilon_2/(2T))}{8\epsilon_2^2(\epsilon_1 + \epsilon_2 - i\omega_n)} \\
&- \frac{\tanh(\epsilon_1/(2T)) - \tanh(\epsilon_2/(2T))}{8\epsilon_2^2(\epsilon_1 - \epsilon_2 - i\omega_n)}
\end{aligned} \tag{41}$$

Now we lower the temperature to critical temperature $T = T_c$ at which there is an onset of superconductivity. To order $1/N$, the condition for T_c is given by

$$K_2(0, 0) + \frac{2T}{N} \sum_{\omega_n} \int \frac{d^d k}{(2\pi)^d} \frac{K_4(k, \omega_n)}{K_2(k, \omega_n)} = 0 \tag{42}$$

We will restrict our analysis of the consequences of Eq. (42) to the balanced case at unitarity, $h = 0$, $\nu = 0$, for which precise Monte Carlo results are also available. This will allow us to test the accuracy of the $1/N$ expansion.

We tabulate the results of some integrals needed for the $1/N$ computation. At $N = \infty$, the transition is obtained by the condition

$$K_2(0, 0) = 0 \quad \Rightarrow \quad \left. \frac{\mu}{T} \right|_{T=T_c} = 1.504476695 \tag{43}$$

All numerical values tabulated below are for the value of μ in Eq. (43) and for $h = 0$, $\nu = 0$.

$$\begin{aligned}
-\frac{dK_2(0, 0)}{d\mu} &= 0.018671(2m)^{3/2}T^{-1/2} \\
T \sum_{\omega_n} \int \frac{d^3 k}{8\pi^3} \frac{K_4(k, \omega_n)}{K_2(k, \omega_n)} &= 0.0263(2m)^{3/2}T^{1/2} \\
2 \int \frac{d^3 k}{8\pi^3} f\left(\frac{k^2}{2m} - \mu\right) &= 0.096549(2mT)^{3/2} \\
2 \frac{d}{d\mu} \int \frac{d^3 k}{8\pi^3} f\left(\frac{k^2}{2m} - \mu\right) &= 0.056179(2m)^{3/2}T^{1/2} \\
-T \sum_{\omega_n} \int \frac{d^3 k}{8\pi^3} \frac{d}{d\mu} \ln[K_2(k, \omega_n)] &= 0.2258(2mT)^{3/2} \\
2T \int \frac{d^3 k}{8\pi^3} \ln(1 + e^{-(k^2/2m - \mu)/T}) &= 0.13188(2m)^{3/2}T^{5/2} \\
-T \sum_{\omega_n} \int \frac{d^3 k}{8\pi^3} \ln[K_2(k, \omega_n)] &= 0.1357(2m)^{3/2}T^{5/2}
\end{aligned} \tag{44}$$

We make a few remarks about the numerical techniques used to obtain the results in Eq. (44). All frequency summations were evaluated on the imaginary frequencies. For all of the expressions, the leading terms at large ω_n , such as terms of order $\ln(\omega_n)$, $1/\omega_n$, $1/\omega_n^{3/2}$,

were obtained explicitly. The summation over these leading terms was performed analytically, along with the required time-splitting convergence factors required for canonical bosons. After subtraction of these leading terms, the summation over the remaining subleading terms was performed numerically, and converged rapidly.

Using the first two results in Eq. (44) and the condition Eq. (42) we obtain the critical chemical potential:

$$\left. \frac{\mu}{T} \right|_{T=T_c} = 1.50448 + \frac{2.785}{N} + \mathcal{O}(1/N^2). \tag{45}$$

The total density of fermions, ρ , is given to order $1/N$ by

$$\frac{\rho}{N} = \int \frac{d^3 k}{8\pi^3} \left[2f\left(\frac{k^2}{2m} - \mu\right) - \frac{T}{N} \sum_{\omega_n} \frac{d}{d\mu} \ln[K_2(k, \omega_n)] \right] \tag{46}$$

As is conventional, we relate ρ to a ‘‘Fermi energy’’, ε_F , by

$$\varepsilon_F = \frac{(3\pi^2 \rho/N)^{2/3}}{2m} \tag{47}$$

Using the third, fourth, and fifth equations in Eq. (44), the value of μ in Eq. (45) and the relations Eq. (46) and (47) we obtain

$$\left. \frac{\varepsilon_F}{T} \right|_{T=T_c} = 2.01424 + \frac{5.317}{N} + \mathcal{O}(1/N^2) \tag{48}$$

Finally, the pressure P is the negative of the grand potential, and so at order $1/N$

$$\begin{aligned}
\frac{P}{N} &= T \int \frac{d^3 k}{8\pi^3} \left[2 \ln(1 + e^{-(k^2/2m - \mu)/T}) \right. \\
&\quad \left. - \frac{T}{N} \sum_{\omega_n} \ln[K_2(k, \omega_n)] \right].
\end{aligned} \tag{49}$$

Using the third and the last two relations in Eq. (44), the value of μ in Eq. (45), and Eq. (49), we obtain

$$\left. \frac{P/N}{(2m)^{3/2}T^{5/2}} \right|_{T=T_c} = 0.13188 + \frac{0.4046}{N} + \mathcal{O}(1/N^2) \tag{50}$$

Although the $1/N$ corrections in Eqs. (45), (48) and (50), are quite large, direct evaluation of the expressions

at $N = 1$ yields values that are in reasonable agreement with recent Monte Carlo results³⁶, which obtained $\mu/T_c = 3.247$, $\varepsilon_F/T_c = 6.579$, and $P/(2m^{3/2}T_c^{5/2}) = 0.776$. The leading $N = \infty$ contributions in the expansion are the contribution of fermion loops, while the $1/N$ corrections come from the boson loops: the distinct physical origins of these contributions indicates that it is not meaningful to compare their values as a test of the accuracy of the expansion. All subsequent $1/N$ contributions are corrections to either the boson or fermion loops, and the agreement with the Monte Carlo results is an encouraging signal that such higher order corrections are indeed small.

1. Relationship to other work

The structure of our leading $1/N$ corrections bears some similarity to the recent work of Haussmann *et al*³⁷. They consider the single fermion loop (our $N = \infty$ terms) and the single boson loop (our $1/N$ corrections) at an equal footing. Thus their approach can be viewed as effectively similar to a self-consistent $1/N$ computation. However, their approach breaks down near T_c , and leads to unphysical results. Near T_c , the value of $K_2(0,0)$ approaches 0, and is also allowed to become negative in a self-consistent approach. Indeed, a direct attempt to obtain T_c by solving Eq. (42) self-consistently for arbitrary N leads immediately to this difficulty: we obtain $K_2(0,0) < 0$ already for $T > T_c$, and the fluctuation propagator in the second term has a negative ‘mass’ and so is obtained by performing a functional integral with an unphysical inverted Gaussian weight. However, organizing the perturbation theory order-by-order in $1/N$ (as we have done) avoids this difficulty, and leads to a well-defined and controlled expansion for the thermodynamic properties at T_c , with all boson loop propagators always obeying $\text{Re}[K_2(k, \omega_n)] \geq 0$.

B. Phase diagram at zero temperature

We will now present some results on the universal phase diagram at $T = 0$. This is determined by 3 parameters: μ , ν , and h . However, these parameters are dimensionful, and the phase diagram can only depend upon *two* independent ratios of these parameters which have zero scaling and engineering dimensions. From Eq. (4), we can deduce that the phase diagram depends upon the ratios of μ , h , and $\nu^2/(2m)$. The sign of h is immaterial, while those of μ and ν are certainly significant, and one or more of these parameters may be zero; consequently we cannot explore the complete phase diagram in a single two-dimensional plot.

First, let us begin with some general considerations at $h = 0$. As long as the detuning, ν , is positive, it will pay to have particles in the ground state of the grand canonical ensemble only for $\mu > 0$. However, for $\nu < 0$,

the negative detuning implies there is a molecular bound state¹⁰ at energy $-\nu^2/m$. So we can expect a non-zero density of particles for $2\mu > -\nu^2/m$. This reasoning led to the phase diagram shown in Fig. 2. We will see shortly that this threshold value of μ is indeed obtained in the $N = \infty$ theory.

For $h \neq 0$, we will limit our analysis here to phases with $\langle \Phi \rangle$ spatially uniform in the $N = \infty$ theory. At $N = \infty$ and $T = 0$, the free energy density in Eq. (37) at $\Lambda = 0$ reduces to:

$$\begin{aligned} \frac{\mathcal{F}}{N} = & \frac{m\nu}{4\pi} |\Phi|^2 - \int \frac{d^3p}{(2\pi)^3} \left[\left(h - \sqrt{\left(\frac{p^2}{2m} - \mu\right)^2 + |\Phi|^2} \right) \right. \\ & \times \theta \left(h - \sqrt{\left(\frac{p^2}{2m} - \mu\right)^2 + |\Phi|^2} \right) \\ & \left. + \sqrt{\left(\frac{p^2}{2m} - \mu\right)^2 + |\Phi|^2} - \left(\frac{p^2}{2m} - \mu\right) - \frac{m|\Phi|^2}{p^2} \right], \end{aligned} \quad (51)$$

where $h > 0$ was assumed without loss of generality. At $h = 0$, we can check for the transition in Fig. 2 by expanding Eq. (51) to order $|\Phi|^2$ for $\mu < 0$. This yields

$$\frac{\mathcal{F}}{N} = |\Phi|^2 \left[\frac{m\nu}{4\pi} - \int \frac{d^3p}{8\pi^3} \left(\frac{1}{2(p^2/(2m) + |\mu|)} - \frac{m}{p^2} \right) \right] + \dots \quad (52)$$

Evaluating the integral, we observe that the co-efficient of $|\Phi|^2$ changes sign at $\mu = -\nu^2/(2m)$, thus establishing the location of the phase boundary in Fig. 2 at $N = \infty$. It is also easy to see that there are no corrections to the position of this phase boundary to all orders in $1/N$: the Φ propagator has spectral weight only at positive frequencies at the phase boundary (including a pole at $\omega = k^2/(4m)$), and this implies that all loop corrections vanish.

Let us now turn to $h \neq 0$. The superfluid phase in Fig. 2 has a gap, equal to $|\Phi|$ (‘spin’ excitations), and consequently a non-zero $|h| \leq |\Phi|$ has no effect on the superfluid phase. The density of the particles remains balanced in this regime, and depends only upon the values of μ and ν .

We show a finite h phase diagram in Fig. 3, obtained by determining the global minimum of the $N = \infty$ free energy in Eq. (51) with respect to variations in a space-independent Φ — a remarkable amount of information emerges from the minimization of this single function. The structure of this universal phase diagram has similarities to that obtained in the resonance-width expansion¹⁴. Because the physics is invariant under the change of sign of h , we plot the phases as a function of the dimensionless parameters $\mu/|h|$ and $\nu/\sqrt{2m|h|}$. In addition to the conventional gapped superfluid state with $|h| < |\Phi|$ and balanced densities, there is also a more exotic superfluid phase in the phase diagram. The Luttinger theorems described in Ref. 38, require that any ground state with an unbalanced density must have at least one Fermi surface (as long as the ‘spin’ rotation symmetry about the

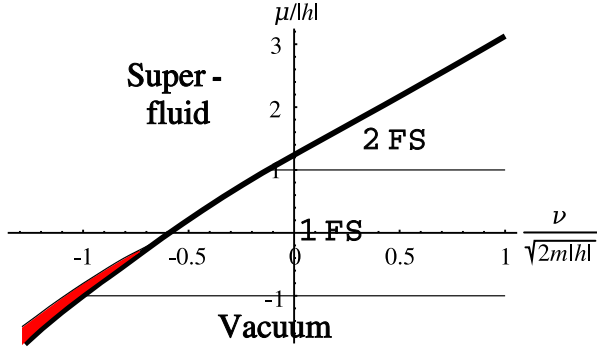


FIG. 3: (color online) Universal phase diagram at $T = 0$, $h \neq 0$, and $N = \infty$. The axes have been scaled by $|h|$ to the dimensionless parameters $\mu/|h|$ and $\nu/\sqrt{2m|h|}$. The density in the superfluid is balanced, except in the shaded (red) region representing a ‘magnetized superfluid’, which also has a single ($1 \times N$) Fermi surface of (say) up spin fermions (for $h > 0$). The 1FS and 2FS phases are non-superfluid states with N and $2N$ Fermi surfaces respectively. The thick line is a first order quantum phase transition, while the thin lines are second order transitions.

‘field’ h , pointing in the z direction in spin space, remains unbroken). The shaded region in Fig 2 is such an unbalanced superfluid phase, which has a single Fermi surface of one of the fermion species (that is, N rather than $2N$) co-existing with the superfluid condensate. Modulated FFLO phases³⁵ have $\langle \Phi \rangle \neq 0$ and space-dependent, and have Fermi surfaces: we briefly discuss such states in Appendix A, but have not yet undertaken the numerical analysis to determine their structure and stability—we will do so in future work.

Other views of the same $N = \infty$ phase diagram are presented in Figs. 4 and 5. The only other stable states we find in our $N = \infty$ theory (with Φ space-independent) are the normal states with $\langle \Phi \rangle = 0$. This appears across a first-order transition indicated by the thick line in Fig. 4. As usual, the existence of this first-order transition as a function of chemical potential means that a system with fixed total density will undergo phase separation. In the present $N = \infty$ theory, one of the phase separated phases will be a superfluid with no population imbalance (fluctuations are not included at $N \rightarrow \infty$). The other phase will be one of the normal states in Fig. 4, which are present for $h > h_c(\nu)$. This normal state has either N or $2N$ Fermi surfaces, depending on whether the external field is strong enough to fully polarize the fermions. The critical field at the Feshbach resonance is $h_c(0) = 0.807125\mu$, and in the range $h_c(0) < h < \mu$ the normal state has $2N$ Fermi surfaces.

It is also interesting to note that the local minimum of free energy at $\Phi \neq 0$ survives at fields h as high as $h_{c2}(\nu)$ shown in Fig. 4 as the dashed line. This local minimum of free energy is global only for $h < h_c(\nu) < h_{c2}(\nu)$. Similarly, the free energy has a local minimum at $\Phi = 0$ for $h > h_{c1}(\nu)$. Therefore, metastable superfluid and normal phases can exist in the range $h_{c1}(\nu) < h < h_{c2}(\nu)$.

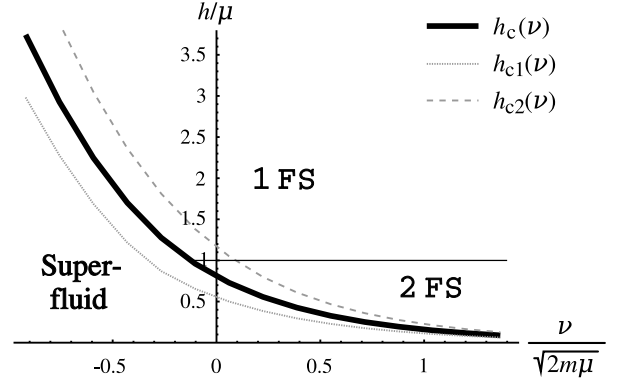


FIG. 4: The same universal, zero temperature phase diagram as in Fig. 3, but for $\mu > 0$. Now we have scaled the axes by μ , and they measure detuning and the field respectively. The first order phase transition between the superfluid and normal phases occurs at $h = h_c(\nu)$, plotted as the thick line; $h_c(0) = 0.807125\mu$. The dashed faint line denotes the ‘upper critical field’ $h_{c2}(\nu)$ (equal to the fermion BCS pairing gap), below which the superfluid may be found at least as a metastable state. Similarly, the dotted faint line denotes the ‘lower critical field’ $h_{c1}(\nu)$, above which the normal state may be found at least as a metastable state.

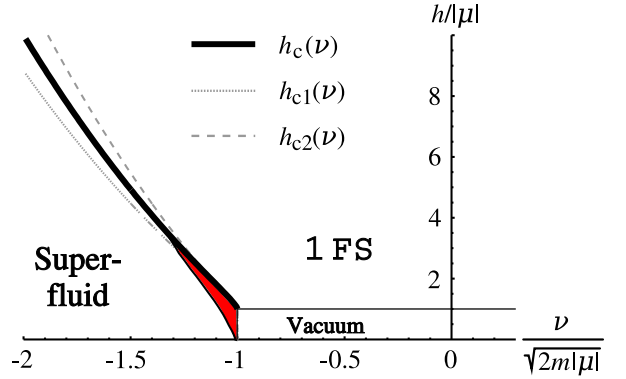


FIG. 5: (color online) As in Fig. 4, but for $\mu < 0$. The shaded (red) region is a ‘magnetized superfluid’.

We now consider $1/N$ corrections to the equation of state of the normal regions of the phase diagram. The pressure is calculated from Eq. (49), which at zero temperature takes the form:

$$\frac{P}{N} = \frac{\mu(2m\mu)^{\frac{3}{2}}}{15\pi^2} \left[\theta \left(1 - \frac{h}{\mu} \right) \left(1 - \frac{h}{\mu} \right)^{\frac{5}{2}} + \theta \left(1 + \frac{h}{\mu} \right) \left(1 + \frac{h}{\mu} \right)^{\frac{5}{2}} \right] + \frac{\delta P}{N}. \quad (53)$$

The calculation of the $1/N$ correction δP is presented in the Appendix B. These $1/N$ corrections are non-zero at $T = 0$ only in the region where both fermion species are present in the ground state *i.e.* in the 2FS state. This state appears only for $\mu > 0$, and so we assume a positive μ below. The scaling form in Eq. (4) implies that

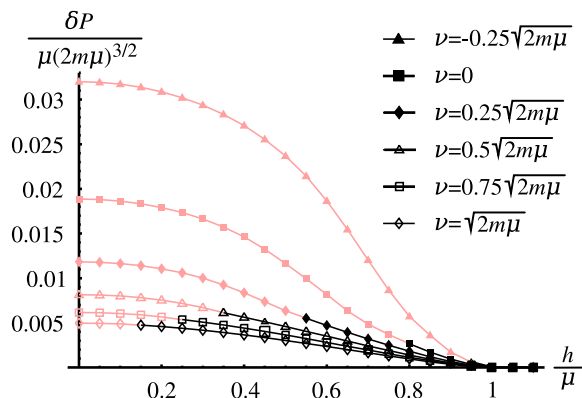


FIG. 6: (color online) $1/N$ correction to pressure in the normal state ($h > h_{c1}(\nu)$) at zero temperature for $\mu > 0$. In the limit $N \rightarrow \infty$ the faded pink portions of the curves should be discarded since they lie within the superfluid phase.

at $T = 0$ this $1/N$ correction can be written in $d = 3$ in the form ($\mu > 0$)

$$\frac{\delta P}{N} = \mu(2m\mu)^{3/2} F_{\delta P} \left(\frac{h}{\mu}, \frac{\nu}{\sqrt{2m\mu}} \right) \quad (54)$$

where $F_{\delta P}$ is a universal function. Our results for the function $F_{\delta P}$ are derived in Appendix B, and plotted in Fig. 6 as a function of h/μ at various values of detuning from the Feshbach resonance. Virtual pairing fluctuations tend to increase pressure, and more so for longer lived pairs. However, for $h > \mu$ the fermion gas is fully polarized and no pairing fluctuations remain to contribute the increase of pressure. Note that the shown δP is valid only when the superfluidity is destroyed. This happens for $h > h_c(\nu)$, which in the case of infinite N corresponds to the dark portions of the curves in the Fig. 6.

The results in Eq. (53) and Fig 6 can have a number of important consequences. Among the most important is that the position of the phase boundaries in Fig. 4 will be moved significantly, especially for negative detuning; additional phases not present at $N = \infty$ could also appear. However, determining this change requires determination of the $1/N$ correction to the energy of the superfluid state: this is a computation similar to that in Appendix B, but more involved because of the broken symmetry in the superfluid state. This computation we also defer to future work, as we discuss further in Section V. Also, the equation of state of the normal state implied by Fig 6 has significant consequences for recent experiments^{28,29}, and these will be described in a separate publication.

V. CONCLUSIONS

This paper has presented a unified understanding of quantum liquids near unitarity in various dimensions us-

ing a renormalization group approach. The universal behavior is associated with RG fixed points describing the interactions of a few ‘atoms’ and ‘molecules’. This fixed point of the zero density theory is⁵ nevertheless a useful and powerful starting point for understanding properties of the quantum liquid with a finite density of particles. We view the RG fixed point as a description of a quantum critical point obtained as the chemical potential of the particles is varied. The quantum (multi-)critical point then describes a quantum phase transition (in the grand canonical ensemble) between a vacuum ground state with zero density of particles, and a finite density quantum liquid; see Fig 2. We have shown how this perspective allows us to bring the standard and well-developed techniques of critical phenomena to the computation of the phase diagram of such liquids.

Our principal application of this method was to the attractive Fermi gas in $d = 3$. The fixed point theory can be described in either a $(d-2)$ or a $(4-d)$ or a $1/N$ expansion (for models with $\text{Sp}(2N)$ symmetry). We argued that the $1/N$ expansion was best suited for the purposes of describing the onset of the non-superconducting ground state with increasing temperature or density imbalance, and presented results to order $1/N$. We also obtained $1/N$ contributions to the equation of state of the normal state.

A number of additional results can be obtained in the $1/N$ expansion, and these we hope to address in separate publications:

- Single particle Green’s functions can also be computed in the $1/N$ expansion by standard methods. In the normal state, these will yield information on the consequences of pairing fluctuations.
- The existence and properties of the modulated FFLO phases are, in principle, also described by universal scaling forms such as Eq. (4). The form of the $N = \infty$ free energy of such phases is discussed in Appendix A, and a numerical analysis of the large parameter space of this result is needed.
- Apart from the existence of FFLO and other phases, the phase boundaries in Fig 4 will also be shifted by $1/N$ corrections, especially in the regime of negative detuning. To compute these, we need the $1/N$ corrections to the free energy in the uniform superfluid phase. This will have an expression which generalizes Eq. (B10) to the broken symmetry phase, and can be computed in a similar manner.
- The equations of state obtained herein, and as indicated above, are expressed in terms of chemical potentials. These can be converted to equations of state as a function of particle densities by standard thermodynamic methods. The local density approximation can then be used to convert the equation of state into particle density profiles in the presence of an external trapping potential.

Acknowledgments

S.S. would like to thank Kun Yang for useful discussions and a previous collaboration on related issues.³⁸ We thank Leo Radzihovsky for valuable comments on the manuscript, for pointing out that a preliminary phase diagram was incomplete, and for informing us about parallel work by M. Veillette, D. Sheehy, and him on the RG approach and the $1/N$ expansion³⁹; where they overlap, our results agree with theirs. We also thank E. Demler, M. Randeria, D. Son, and M. Zwierlein for useful discussions. This research was supported by the NSF under grant DMR-0537077. We thank Aspen Center for Physics for hospitality.

APPENDIX A: $N = \infty$ THEORY FOR FFLO STATES

This appendix generalizes the $N = \infty$ result in Eq. (37) to states with a spatially dependent Φ .

We expect that the optimum solution for $\Phi(x)$ will have the symmetry of some Bravais lattice, and so write

$$\Phi(x) = \sum_{\mathbf{G}} \Phi_{\mathbf{G}} e^{i\mathbf{G}\cdot\mathbf{x}} \quad (\text{A1})$$

where \mathbf{G} are the reciprocal lattice vectors. First, we need the energy eigenvalues of the Bogoliubov-de Gennes equations in the presence of such a $\Phi(x)$. We can expand the eigenmodes ($u(x), v(x)$) also in plane-wave Bloch eigenstates

$$u(x) = e^{i\mathbf{p}\cdot\mathbf{x}} \sum_{\mathbf{G}} u_{\mathbf{G}} e^{i\mathbf{G}\cdot\mathbf{x}}, \quad (\text{A2})$$

and similarly for $v(x)$. Then the eigenvalue equation is

$$\begin{aligned} \left(\frac{(\mathbf{p} + \mathbf{G})^2}{2m} - \mu \right) u_{\mathbf{G}} + \sum_{\mathbf{G}'} \Phi_{\mathbf{G}-\mathbf{G}'} v_{\mathbf{G}'} &= \epsilon_{\mathbf{p}}(\Phi) u_{\mathbf{G}} \\ - \left(\frac{(\mathbf{p} + \mathbf{G})^2}{2m} - \mu \right) v_{\mathbf{G}} + \sum_{\mathbf{G}'} \Phi_{\mathbf{G}-\mathbf{G}'}^* u_{\mathbf{G}'} &= \epsilon_{\mathbf{p}}(\Phi) v_{\mathbf{G}}, \end{aligned}$$

where $\epsilon_{\mathbf{p}}(\Phi)$ are the Bloch eigenenergies. We now have to choose a truncation of the set of reciprocal lattice vectors, and then numerically diagonalize the equations above to obtain these eigenenergies. An infinite set of positive eigenenergies will be obtained for each \mathbf{p} in the first Brillouin zone. In an extended zone scheme, these eigenenergies can be rearranged to obtain a single-valued and positive function of \mathbf{p} , $\epsilon_{\mathbf{p}}(\Phi)$, where \mathbf{p} extends over all real values in d -dimensional momentum space. This function can be chosen so that for Φ constant, $\epsilon_{\mathbf{p}}(\Phi) = ((p^2/(2m) - \mu)^2 + |\Phi|^2)^{1/2}$.

Now, it is easy to see that the generalization of Eq. (36)

is

$$\begin{aligned} \frac{\mathcal{F}^{(0)}}{N} &= \frac{m\nu}{4\pi} \sum_{\mathbf{G}} |\Phi_{\mathbf{G}}|^2 - \int \frac{d^3p}{(2\pi)^3} \left[\right. \\ &T \ln \left(1 + e^{-(\epsilon_{\mathbf{p}}(\Phi)-h)/T} \right) + T \ln \left(1 + e^{-(\epsilon_{\mathbf{p}}(\Phi)+h)/T} \right) \\ &\left. + \epsilon_{\mathbf{p}}(\Phi) - \left(\frac{p^2}{2m} - \mu \right) \right]. \quad (\text{A3}) \end{aligned}$$

where the integral is over all momenta. As in Eq. (36) this expression suffers from an ultraviolet divergence, and we cure this by dimensional regularization. At large p , the values of $\epsilon_{\mathbf{p}}(\Phi)$ can be obtained by perturbation theory in Φ , and the divergent pieces only involve terms to second order in Φ . Adding and subtracting this divergent term to Eq. (A3), and analytically performing the dimensional regularization as in Eq. (37) at $\Lambda = 0$, we obtain

$$\begin{aligned} \frac{\mathcal{F}}{N} &= \frac{m\nu}{4\pi} \sum_{\mathbf{G}} |\Phi_{\mathbf{G}}|^2 - \int \frac{d^3p}{(2\pi)^3} \left[\right. \\ &T \ln \left(1 + e^{-(\epsilon_{\mathbf{p}}(\Phi)-h)/T} \right) + T \ln \left(1 + e^{-(\epsilon_{\mathbf{p}}(\Phi)+h)/T} \right) \\ &\left. + \epsilon_{\mathbf{p}}(\Phi) - \left(\frac{p^2}{2m} - \mu \right) - \frac{m}{p^2} \sum_{\mathbf{G}} |\Phi_{\mathbf{G}}|^2 \right]. \quad (\text{A4}) \end{aligned}$$

It now remains to numerically minimize Eq. (A4) over the set of values of $\Phi_{\mathbf{G}}$.

APPENDIX B: EQUATION OF STATE AT $T = 0$

Here we present some details regarding the $1/N$ corrections to the equation of state in the absence of condensate at zero temperature. These corrections appear only in the normal states with two ($2 \times N$) Fermi surfaces, so that we assume $\mu > 0$. The equation of state up to the order of $1/N$ is generally obtained from Eq. (49) generalized to finite external fields h .

At $T = 0$ and in the absence of condensate it is possible to analytically calculate K_2 . Consider first the imaginary part of Eq. (39) after analytic continuation to real frequencies $i\omega \rightarrow \omega + i0^+$:

$$\begin{aligned} -\frac{1}{\pi} \text{Im}\{K_2(k, \omega)\} &= \int \frac{d^3p}{(2\pi)^3} \left[1 - \theta \left(h - \frac{p^2}{2m} + \mu \right) \right. \\ &\left. - \theta \left(-h - \frac{(\mathbf{p} + \mathbf{k})^2}{2m} + \mu \right) \right] \times \\ &\delta \left(\omega + 2\mu - \frac{p^2}{2m} - \frac{(\mathbf{p} + \mathbf{k})^2}{2m} \right). \quad (\text{B1}) \end{aligned}$$

Note that in the rest of this appendix we will denote by $K_2(k, \omega)$ the dependence on *real* frequency ω , which is a slight change of notation from Eq. (39). Upon the shift

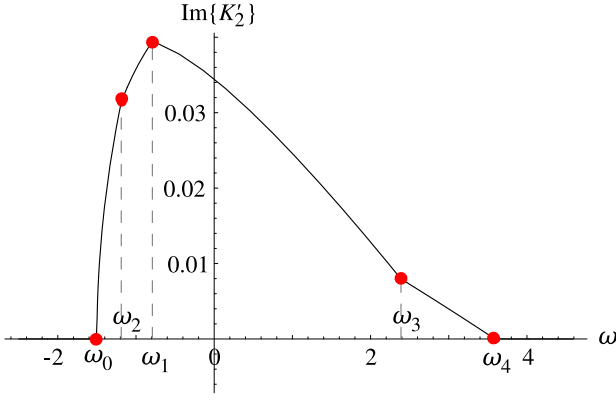


FIG. 7: (color online) A typical plot of $\text{Im}\{K'_2(k, \omega)\}$ versus frequency (here $\mu = 1$, $m = 0.5$, $h = 0.2$, $k = 1$). There are up to five kink frequencies, listed in (B8), including the end-points. $\text{Im}\{K'_2(k, \omega)\}$ is non-zero only in a finite interval.

of variables $\mathbf{p} \rightarrow \mathbf{p} - \mathbf{k}/2$, the delta function fixes the magnitude of \mathbf{p} :

$$p = p(k, \omega) \equiv \sqrt{m(2\mu + \omega) - \frac{k^2}{4}}, \quad (\text{B2})$$

while the remaining integral over spatial direction of \mathbf{p} is carried out easily:

$$\text{Im}\{K_2(k, \omega)\} = \text{Im}\{K'_2(k, \omega)\} - \frac{mp}{4\pi}\theta(p^2) \quad (\text{B3})$$

where

$$\begin{aligned} \text{Im}\{K'_2(k, \omega)\} &= \frac{mp}{8\pi}\theta(p^2) \\ &\times \left[R\left(\frac{m(\omega + 2h)}{pk}\right) + R\left(\frac{m(\omega - 2h)}{pk}\right) \right], \end{aligned} \quad (\text{B4})$$

and

$$R(x) = \begin{cases} 2 & , x \leq -1 \\ 1 - x & , -1 \leq x \leq 1 \\ 0 & , x \geq 1 \end{cases}. \quad (\text{B5})$$

The real part of $K_2(k, \omega)$ can be obtained from the requirement that K_2 be analytic in the upper complex half-plane of ω . Hence, the Kramers-Kronig relations will be

useful, but they can be applied only to the well behaved portion $K'_2(k, \omega)$. Fortunately, it is easy to recognize that the portion of $K_2(k, \omega)$ whose imaginary part diverges when $\omega \rightarrow \infty$ (the second term in (B3)) is just a square root function:

$$\begin{aligned} \frac{m}{4\pi} \sqrt{\frac{k^2}{4} - m(2\mu + \omega + i0^+)} &= \\ \frac{m\sqrt{-p^2}}{4\pi} \theta(-p^2) - i \frac{mp}{4\pi} \theta(p^2). \end{aligned} \quad (\text{B6})$$

We now determine the real part of $K'_2(k, \omega)$ using the Kramers-Kronig relation:

$$\text{Re}\{K'_2(k, \omega)\} = \frac{1}{\pi} \int_{-\infty}^{\infty} d\omega' \frac{\mathbb{P}}{\omega' - \omega} \text{Im}\{K'_2(k, \omega')\}. \quad (\text{B7})$$

A typical plot of $\text{Im}\{K'_2(k, \omega)\}$ is shown in Fig. 7. Depending on the values of μ , h and k there are up to five frequencies where $\text{Im}\{K'_2(k, \omega)\}$ has kinks:

$$\begin{aligned} \omega_0 &= \frac{k^2}{4m} - 2\mu \\ \omega_1 &= \omega_0 + \frac{1}{m} \left(\frac{k}{2} - \sqrt{2m(\mu + h)} \right)^2 \\ \omega_2 &= \omega_0 + \frac{1}{m} \left(\frac{k}{2} - \sqrt{2m(\mu - h)} \right)^2 \\ \omega_3 &= \omega_0 + \frac{1}{m} \left(\frac{k}{2} + \sqrt{2m(\mu - h)} \right)^2 \\ \omega_4 &= \omega_0 + \frac{1}{m} \left(\frac{k}{2} + \sqrt{2m(\mu + h)} \right)^2. \end{aligned} \quad (\text{B8})$$

We evaluate the integral (B7) piecewise between these kink frequencies. Knowing both the real and imaginary parts of $K'_2(k, \omega)$ for real frequencies, together with (B3) and (B6), allows reconstruction of the full function $K_2(k, \omega)$, analytic in the upper complex half-plane of ω :

$$\begin{aligned}
K_2(k, \omega) = & \frac{m\nu}{4\pi} + \frac{m}{4\pi} \sqrt{\frac{k^2}{4} - m(2\mu + \omega)} \\
& + \frac{m}{4\pi^2} \theta(\mu + h) \left\{ \theta \left(2m(\mu + h) - \frac{k^2}{4} \right) \left[2p(\omega_1) + p(\omega) \ln \left(-\frac{p(\omega_1) - p(\omega)}{p(\omega_1) + p(\omega)} \right) \right] \right. \\
& - \frac{p(\omega)}{2} \left[\ln \left(\frac{p(\omega_4) + p(\omega)}{p(\omega_4) - p(\omega)} \right) - \ln \left(\frac{p(\omega_1) + p(\omega)}{p(\omega_1) - p(\omega)} \right) \right] + p(\omega_4) - p(\omega_1) - \frac{m}{2k} \left[\omega_4 - \omega_1 + (\omega - 2h) \ln \left(\frac{\omega_4 - \omega}{\omega_1 - \omega} \right) \right] \left. \right\} \\
& + \frac{m}{4\pi^2} \theta(\mu - h) \left\{ \theta \left(2m(\mu - h) - \frac{k^2}{4} \right) \left[2p(\omega_2) + p(\omega) \ln \left(-\frac{p(\omega_2) - p(\omega)}{p(\omega_2) + p(\omega)} \right) \right] \right. \\
& - \frac{p(\omega)}{2} \left[\ln \left(\frac{p(\omega_3) + p(\omega)}{p(\omega_3) - p(\omega)} \right) - \ln \left(\frac{p(\omega_2) + p(\omega)}{p(\omega_2) - p(\omega)} \right) \right] + p(\omega_3) - p(\omega_2) - \frac{m}{2k} \left[\omega_3 - \omega_2 + (\omega + 2h) \ln \left(\frac{\omega_3 - \omega}{\omega_2 - \omega} \right) \right] \left. \right\}
\end{aligned} \tag{B9}$$

Here, $p(\omega)$ is given by (B2), where dependence on k is assumed and omitted for brevity.

Now we can calculate the $1/N$ correction to pressure in the normal state at zero temperature. For this purpose we substitute (B9) into (49):

$$\frac{\delta P}{N} = -\frac{1}{N} \int \frac{d^3 k}{(2\pi)^3} \int_{-\infty}^{\infty} \frac{d\omega}{2\pi} e^{i\omega 0^+} \ln [K_2(k, i\omega)] . \tag{B10}$$

The change of variables $i\omega \rightarrow \omega$ allows the frequency integral to be evaluated on the closed path in complex plane shown in Fig. 8. Avoiding the branch-cut of the logarithm, and exploiting the analyticity of $K_2(k, \omega)$, the

integral above reduces to:

$$\begin{aligned}
\frac{\delta P}{N} &= \frac{i}{N} \int \frac{d^3 k}{(2\pi)^3} \int_{-\infty}^0 \frac{d\omega}{2\pi} \ln \left(\frac{K_2(k, \omega - i0^+)}{K_2(k, \omega + i0^+)} \right) \tag{B11} \\
&= \frac{1}{N} \frac{1}{2\pi^3} \int_0^{\infty} dk \int_{-\infty}^0 d\omega k^2 \arg [K_2(k, \omega + i0^+)] .
\end{aligned}$$

In the second line we have used the fact that $K_2(k, \omega - i0^+) = K_2^*(k, \omega + i0^+)$. This integral has to be evaluated numerically. The plot of pressure correction at zero temperature is shown in Fig. 6.

- ¹ M. Girardeau, J. Math. Phys. **1**, 516 (1960); E. Lieb and W. Liniger, Phys. Rev. **130**, 1605 (1963); F. D. M. Haldane, Phys. Rev. Lett. **47**, 1840 (1981).
- ² V. E. Korepin, N. M. Bogoliubov, A. G. Izergin, and P. V. Landshoff, *Quantum Inverse Scattering Method and Correlation Functions*, Cambridge University Press, Cambridge (1993).
- ³ K. Damle and S. Sachdev, Phys. Rev. Lett. **76**, 4412 (1996).
- ⁴ S. Sachdev and A. P. Young, Phys. Rev. Lett. **78**, 2220 (1997).
- ⁵ S. Sachdev, *Quantum Phase Transitions*, Cambridge University Press, Cambridge (1999), Chapter 11.
- ⁶ B. Paredes, A. Widera, V. Murg, O. Mandel, S. Fölling, I. Cirac, G. V. Shlyapnikov, T. Hänsch, and I. Bloch, Nature **429**, 277 (2004).
- ⁷ G. Bertsch, *Many-Body X Challenge*, in: Proc. X Conference on Recent Progress in Many-Body Theories, eds. R. F. Bishop *et al.* (World Scientific, Singapore, 2000).
- ⁸ T.-L. Ho, Phys. Rev. Lett. **92**, 090402 (2004).
- ⁹ J. Stewart, J. P. Gaebler, C. A. Regal, and D. S. Jin, cond-mat/0607776.
- ¹⁰ R. A. Duine and H. T. C. Stoof, Phys. Rep. **396**, 115 (2004).

- ¹¹ E. B. Kolomeisky and J. P. Straley, Phys. Rev. B **46**, 11749 (1992).
- ¹² S. Sachdev, T. Senthil, and R. Shankar, Phys. Rev. B **50**, 258 (1994).
- ¹³ A. V. Andreev, V. Gurarie, and L. Radzihovsky, Phys. Rev. Lett. **93**, 130402 (2004).
- ¹⁴ D. E. Sheehy and L. Radzihovsky, Phys. Rev. Lett. **96**, 060401 (2006); cond-mat/0607803, cond-mat/0608172.
- ¹⁵ C.-H. Pao and S.-T. Wu, S.-K. Yip, Phys. Rev. B **73**, 132506 (2006); cond-mat/0608501.
- ¹⁶ S. Diehl and C. Wetterich, Phys. Rev. A **73**, 033615 (2006).
- ¹⁷ D. S. Fisher and P. C. Hohenberg Phys. Rev. B **37**, 4936 (1988); M. P. A. Fisher, P. B. Weichmann, G. Grinstein, and D. S. Fisher, Phys. Rev. B **40**, 546 (1989).
- ¹⁸ E. Brezin, J. C. Le Guillou and J. Zinn-Justin, in *Phase Transitions and Critical Phenomena*, vol. 6, C. Domb and M. S. Green eds., Academic Press, London (1976).
- ¹⁹ F. Sauli and P. Kopietz, cond-mat/0608423.
- ²⁰ P. Nozières and S. Schmitt-Rink, J. Low Temp. Phys. **59**, 195 (1985).
- ²¹ C. A. R. Sá de Melo, M. Randeria, and J. R. Engelbrecht, Phys. Rev. Lett. **71**, 3202 (1993).
- ²² Q. Chen, I. Kosztin, and K. Levin, Phys. Rev. Lett. **85**, 2801 (2000).

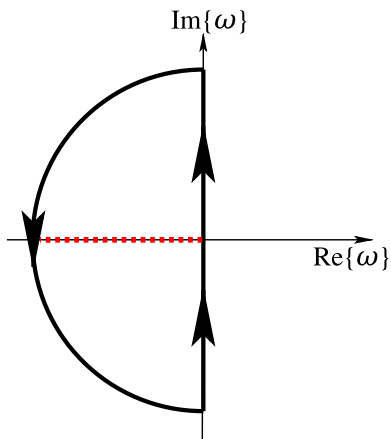


FIG. 8: (color online) The complex path of ω along which $\ln K_2(k, \omega)$ is integrated out in (B10) (the radius of the semi-circle is infinite). The dashed red line shows the branch-cut of the logarithm.

- ²³ Y. Ohashi and A. Griffin, Phys. Rev. Lett. **89**, 130402 (2002).
²⁴ E. Timmermans K. Furuya, P. W. Milonni, and A. K. Kerman, Phys. Lett. A **285**, 228 (2001); M. Holland, S. J. J. M. F. Kokkelmans, M. L. Chiofalo, and R. Walser, Phys. Rev. Lett. **87**, 120406 (2001).
²⁵ Y. Nishida and D. T. Son, Phys. Rev. Lett. **97**, 050403 (2006); Y. Nishida, cond-mat/0608321; P. Arnold, J. E. Drut, D. T. Son, cond-mat/0608477.
²⁶ Z. Nussinov and S. Nussinov, cond-mat/0410597.

- ²⁷ Y. Nishida and D. T. Son, cond-mat/0607835.
²⁸ M. W. Zwierlein, A. Schirotzek, C. H. Schunck, and W. Ketterle, Science **311**, 492 (2006); Y. Shin, M. W. Zwierlein, C. H. Schunck, A. Schirotzek, and W. Ketterle, Phys. Rev. Lett. **97**, 030401 (2006).
²⁹ G. B. Partridge, W. Li, R. I. Kamar, Y. Liao, and R. G. Hulet, Science **311**, 503 (2006); G. B. Partridge, W. Li, Y. A. Liao, R. G. Hulet, M. Haque, and H. T. C. Stoof, cond-mat/0608455.
³⁰ S. Sachdev and Z. Wang, Phys. Rev. B **43**, 10229 (1991); S. Sachdev and N. Read, Int. J. Mod. Phys. B **5**, 219 (1991) (cond-mat/0402109).
³¹ V. Gurarie, Phys. Rev. A **73**, 033612 (2006).
³² S. Powell, S. Sachdev, and H. P. Büchler, Phys. Rev. B **72**, 024534 (2005).
³³ M. W. J. Romans, R. A. Duine, S. Sachdev, and H. T. C. Stoof, Phys. Rev. Lett. **93**, 020405 (2004).
³⁴ See, for example, “An Introduction to Quantum Field Theory” by M. E. Peskin, D. V. Schroeder; Perseus Books, Cambridge, Massachusetts (1995).
³⁵ P. Fulde and R. A. Ferrell, Phys. Rev. **135**, A550 (1964). A. I. Larkin and Yu. N. Ovchinnikov, Zh. Eksp. Teor. Fiz **47**, 1136 (1964) [Sov. Phys. JETP **20**, 762 (1965)].
³⁶ E. Burovski, N. Prokof’ev, B. Svistunov, and M. Troyer, Phys. Rev. Lett. **96**, 160402 (2006) and cond-mat/0605350.
³⁷ R. Haussmann, W. Rantner, S. Cerrito, and W. Zwerger, cond-mat/0608282.
³⁸ K. Yang and S. Sachdev, Phys. Rev. Lett. **96**, 187001 (2006); S. Sachdev and K. Yang, Phys. Rev. B **73**, 174504 (2006).
³⁹ M. Y. Veillette, D. E. Sheehy, and L. Radzihovsky, cond-mat/0610798.